Population robustness arising from cellular heterogeneity

Pawel Paszek[a], Sheila Ryan[a], Louise Ashall[a], Kate Sillitoe[a], Claire V. Harper[a], David G. Spiller[a], David A. Rand[b], and Michael R. H. White[a,1]

[a]Centre for Cell Imaging, School of Biological Sciences, University of Liverpool, Liverpool L69 7ZB, United Kingdom; and [b]Warwick Systems Biology and Mathematics Institute, University of Warwick, Coventry CV4 7AL, United Kingdom

Edited by Avner Friedman, The Ohio State University, Columbus, OH, and approved April 14, 2010 (received for review December 4, 2009)

Heterogeneity between individual cells is a common feature of dynamic cellular processes, including signaling, transcription, and cell fate; yet the overall tissue level physiological phenotype needs to be carefully controlled to avoid fluctuations. Here we show that in the NF-κB signaling system, the precise timing of a dual-delayed negative feedback motif [involving stochastic transcription of inhibitor κB (IκB)-α and -ε] is optimized to induce heterogeneous timing of NF-κB oscillations between individual cells. We suggest that this dual-delayed negative feedback motif enables NF-κB signaling to generate robust single cell oscillations by reducing sensitivity to key parameter perturbations. Simultaneously, enhanced cell heterogeneity may represent a mechanism that controls the overall coordination and stability of cell population responses by decreasing temporal fluctuations of paracrine signaling. It has often been thought that dynamic biological systems may have evolved to maximize robustness through cell-to-cell coordination and homogeneity. Our analyses suggest in contrast, that this cellular variation might be advantageous and subject to evolutionary selection. Alternative types of therapy could perhaps be designed to modulate this cellular heterogeneity.

network topology | NF-κB | biological oscillations | feedback regulation | paracrine signaling

A key question is how biological function emerges from a dynamic population of cells when high levels of cellular heterogeneity are often observed. The overall tissue-level phenotype arising from the cell population average needs to be carefully controlled. Noise originates from stochastic processes when there are low numbers of molecules, such as in transcription, where there are normally only two copies of each gene per cell (1–3). It has generally been thought that tissue-level control requires cells to form a relatively homogeneous population. Such homogeneity could arise either from a high probability of individual cells being in the same state or from positive feedback coordination through cell-to-cell paracrine signaling entraining the dynamic responses of the cell population (4). For example, individual neurons lose circadian clock synchrony when separated from each other, but the intact tissue shows a robust and precise 24-h rhythm (5, 6).

The NF-κB family of transcription factors critically regulates innate immunity and inflammation and has a key role in cell division and cell death (7). NF-κB must rapidly decode extracellular signals and encode intracellular information to regulate individual cell fate decisions (8, 9). NF-κB also regulates the production and secretion of cytokines that play a key role in amplification and propagation of inflammatory responses (10, 11). Therefore, the overall population response to a given dynamic stimulus requires precise spatial and temporal control.

We previously applied time-lapse single cell imaging to show that NF-κB signaling in response to TNFα stimulation involves oscillations of the transcription factor between cytoplasm and the nucleus of cells (12–14). This behavior is maintained in mouse embryonic fibroblasts (MEFs) from transgenic animals (15). Like Ca^{2+} signaling (16), the frequency of NF-κB oscillations coordinates differential gene expression (12). This suggests that the maintenance of robust oscillations is a fundamental functional property of the NF-κB system. Although the initial response is synchronized, the later oscillations are asynchronous between cells and therefore are not readily discerned by population level analyses (17, 18). A three-feedback stochastic model of the NF-κB system was applied to show that the variation in NF-κB dynamics may arise through stochastic transcription of negative feedback genes, including inhibitor κB (IκB)-α, A20 and especially IκBε (12), which was thought to be particularly relevant (19). TNFα-induced transcription of IκBε has been found to be delayed relative to IκBα by around 45 min (12, 18), creating a characteristic dual negative feedback motif (20) (Fig. 1*A*) in the network structure. We suggested that this IκB motif gives rise to substantial cell-to-cell heterogeneity (12). In support of this theoretical prediction, it has been shown that MEF cells lacking IκBε show enhanced oscillation dynamics in DNA binding at the cell population level (18). We propose that this arises from enhanced cell-to-cell oscillation synchrony (12).

Results

Timing of the Dual Negative IκB Feedback Motif Is Stimulus-Dependent. In the present study, we examined the kinetics of IκBα and IκBε activation by quantitative RT-PCR in MEF and SK-N-AS (human S-type neuroblastoma) cells in response to three stimuli that could induce single-cell NF-κB oscillations (Fig. S1). In both cell lines, transcription of IκBε was delayed with respect to that of IκBα in response to the proinflammatory cytokines TNFα and interleukin 1 beta (IL-1β), but not phorbol ester differentiation factor phorbol 12-myristate 13-acetate (PMA) (Fig. 1 *B–D* and Fig. S2). Although the IκBα transcript level increased immediately after stimulation with either TNFα or IL-1β, reaching its maximum as early as at 30 min in response to IL-1β, IκBε showed no response before 35 min and a maximum at about 120 min after either treatment. The gradual population-level increase of IκBε mRNA between 30 and 60 min after stimulation suggested that, although showing a consistent 45-min average time delay in IκBε transcription (12, 18), this delay might vary significantly between individual cells, perhaps due to a stochastic initiation of transcription. In contrast, PMA treatment showed a relatively delayed transcription of both IκBα and IκBε genes so that both feedback arms were activated concordantly about 45 min after stimulation (Fig. 1*D* and Fig. S2*C*). These data suggested that an important component of the NF-κB signaling network, the timing of the double negative IκB feedback, is stimulus-dependent.

Author contributions: P.P., S.R., L.A., K.S., C.V.H., D.G.S., D.A.R., and M.R.H.W. designed research; P.P., S.R., L.A., K.S., and C.V.H. performed research; P.P., S.R., L.A., K.S., and C.V.H. analyzed data; and P.P., D.G.S., D.A.R., and M.R.H.W. wrote the paper.

The authors declare no conflict of interest.

This article is a PNAS Direct Submission.

Freely available online through the PNAS open access option.

[1]To whom correspondence should be addressed. E-mail: mwhite@liv.ac.uk.

This article contains supporting information online at www.pnas.org/lookup/suppl/doi:10.1073/pnas.0913798107/-/DCSupplemental.

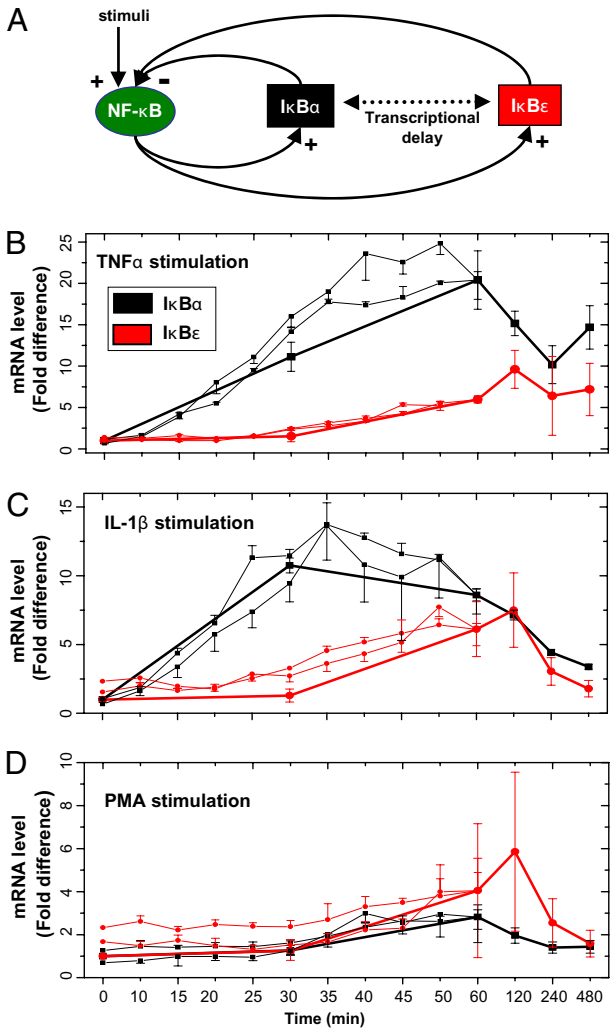

Fig. 1. Transcriptional regulation of dual negative IκB feedback. (*A*) Schematic representation of the dual negative IκB feedback motif showing the time delay between activation of IκBα and IκBε transcription. (*B–D*) Quantitative RT-PCR analysis of IκBα and IκBε mRNA levels in mouse embryonic fibroblasts (MEF) cells stimulated with (*B*) 10 ng/mL TNFα, (*C*), 10 ng/mL IL-1β and (*D*) 100 μM PMA. Thick lines depict stimulation over a 480-min time course. Results (1 replicate) were normalized to unstimulated controls (in triplicates). Error bars (1 SD) were calculated by propagating the error from the unstimulated controls. Thin lines represent stimulation over 60-min time course (two replicates) normalized to the former at the 60-min time point.

IκB Feedback Motif Controls Heterogeneity of NF-κB Oscillation Timing Between Individual Cells. To theoretically investigate how the network topology contributes to the dynamic properties of NF-κB signaling, we constrained the structure (21) (Fig. S3, Tables S1 and S2) and parameters (Table S3) of a previously described stochastic model (12) and fitted to population data obtained from MEF cells (*SI Appendix*). We assumed that kinetic differences between the IκBα and IκBε isoforms originated from their transcriptional regulation. This model closely recapitulated the experimental data (nuclear NF-κB, total IκBα, IκBε, and A20 protein and mRNA, and IκB kinase (IKK) activity levels) obtained under a series of genetic conditions (WT, IκBα$^{-/-}$, IκBε$^{-/-}$ and A20$^{-/-}$) and stimulation protocols (chronic and pulses of TNFα of varying duration and frequency) (12, 17, 18, 22–24) (Figs. S4, S5, S6, S7 and S8). The comparison between simulations and previously published experimental data from populations of WT and IκBε knock-out MEFs (18) showed a qualitative change in system dynamics (damped vs. persistent oscillations, respectively), which depended on the network topology (Fig. S4). In agreement with simulations from our previous model (12), we found that these population level responses were determined by the heterogeneity of single cell oscillations and orchestrated through the dual negative IκB feedback motif (Fig. 2*A* and Figs. S9 and S10). The 45-min transcriptional delay between activation of redundant IκBα and IκBε feedback loops did not substantially change the average timing or amplitude of NF-κB oscillations but specifically affected heterogeneity in the cell-to-cell timing (and therefore phasing of the oscillations) (Fig. 2*B* and Fig. S11). Ablation of the IκBε negative feedback therefore resulted in increased cell-to-cell homogeneity of oscillation timing and elicited more persistent population-level NF-κB oscillations.

Timing of IκBε Transcriptional Delay Is Optimal for Inducing Cellular Heterogeneity. Given the apparent key role of the delayed IκBε feedback loop for the generation of cell-to-cell heterogeneity, we tested the effect of altering the timing of the IκBε delay on the emergent dynamics of the system (Fig. S12). This analysis showed that the 45-min IκBε transcription delay is optimal for generation of cellular variation in oscillation timing. A substantial decrease in heterogeneity (shown as the nuclear NF-κB peak3 to peak4 oscillation timing Fano factor: variance normalized by mean timing) to a level comparable to complete removal of the IκBε feedback loop was observed when the IκBε time-delay was increased or decreased by as little as 15 min (Fig. 3*A*). If this delay was varied further, the cells became even more synchronous. The heterogeneity was still maximized when

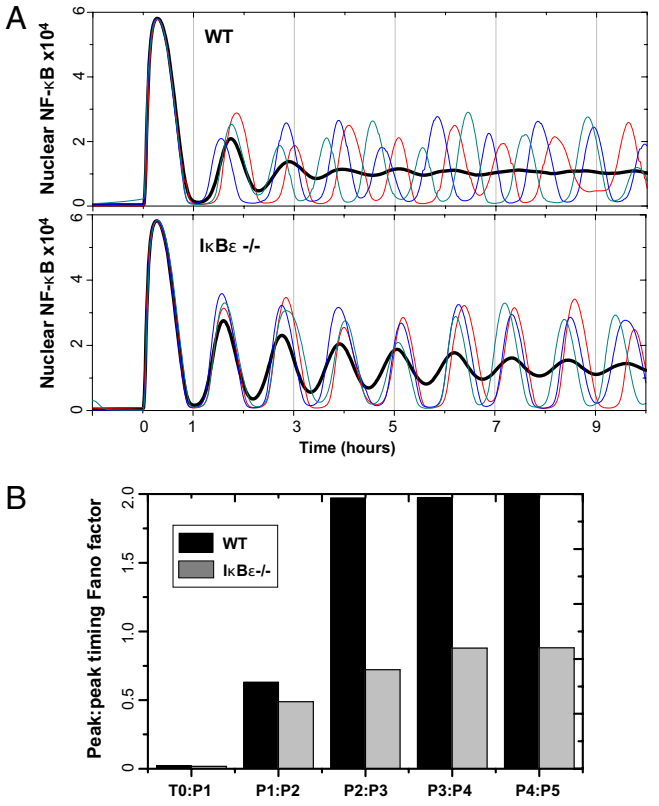

Fig. 2. Delay-induced heterogeneity of NF-κB oscillation timing. (*A*) Simulated nuclear NF-κB kinetics following chronic TNFα stimulation of WT and IκBε knock-out (IκBε$^{-/-}$) cells. Three single cell trajectories are shown with colored lines. The population average constructed from 500 cells is shown with a thick black line. (*B*) Analysis of single cell oscillation timing based on data in *A*. Variability is represented by Fano factor (variance normalized by average) of peak-to-peak timing.

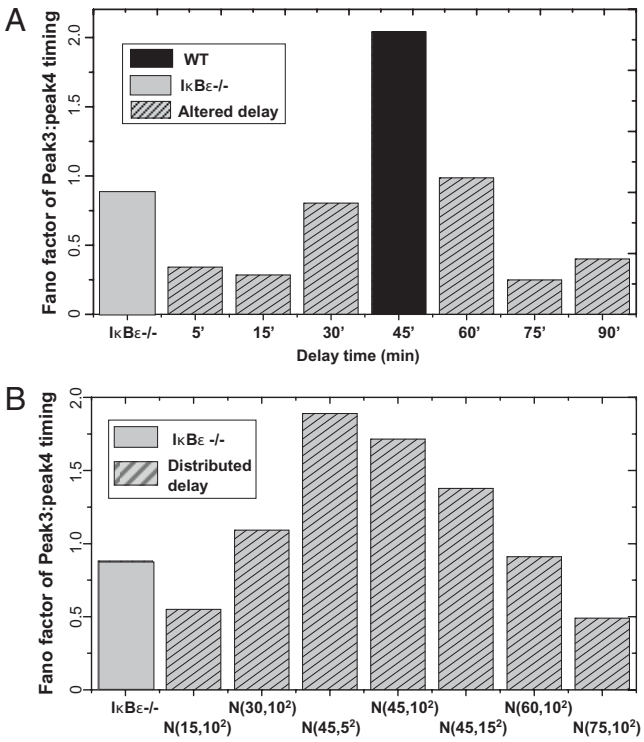

Fig. 3. IκBε transcriptional delay maximizes heterogeneity between individual cells. (*A*) Effect of the altered delay time. Fano-factor for nuclear NF-κB peak3-to-peak4 timing, based on 200 single cells simulated for 5-, 15-, 30-, 45- (WT), 60-, 75-, and 90-min transcriptional delay and IκBε-deficient cells (Fig. S12). (*B*) Effect of the distributed delay time. Fano-factor for nuclear NF-κB peak3-to-peak4 timing, based on 2,000 single cells simulated for distributed IκBε delay time vs. IκBε knock-out. The delay time was randomized according to a normal distribution with mean μ (min.) and SD σ, N (μ, σ^2), in a population, but constant per cell (Fig. S13).

the delay time in the population was distributed around 45 min (Fig. 3*B* and Fig. S13). The heterogeneity of the NF-κB oscillation timing is proposed to originate from stochastic processes driven by the transcriptional activation of individual feedback genes (*SI Appendix*). The model suggests that the optimal time-lag between the two IκB feedback loops results in substantially increased variability because of the contribution of stochastic noise from each feedback loop (Fig. 3*A*). When the two feedbacks operated more in phase (with suboptimal delay), the coincidence of the two negative feedback loops reinforced homogeneity, leading to more synchronized cell dynamics.

IκBε Feedback Maintains Robust Single-Cell NF-κB Oscillations. We next compared the ability of WT and IκBε knock-out conditions to maintain oscillations. We previously showed experimentally that the persistence, amplitude, and oscillation period in WT cells was not affected by the NF-κB level (25). A detailed analysis of the peak-to-peak timing over an 18-fold range in NF-κB expression level predicted that IκBε knock-out cells exhibited a much larger sensitivity to the NF-κB expression level than WT cells (Fig. 4*A* and Fig. S14). Above an approximately 2.5-fold expression level, oscillations in IκBε-deficient cells ceased, whereas oscillations in WT cells for equivalent and higher expression levels were maintained (Fig. S15). To test the response to other perturbations to the system, we also varied each of the model parameters by two-fold (Fig. S16, Fig. S17, Fig. S18 and Fig. S19) and analyzed selected features (peak amplitude and periodicity) of single cell NF-κB oscillations (*SI Appendix*). We found that a group of key parameters (*c1a*, *c2a, c3a, kc2a, c1*, *c2*, *c4, kp*, *ki*, *kii*) (Table S3) related to levels of IκBα, A20, and IKK activity controlled NF-κB kinetics in both WT (26) and IκBε knock-out cells (Fig. S20). Importantly, the IκBε knock-out condition showed substantially increased sensitivity to single parameter changes for all oscillatory features, compared with WT (Fig. 4 *B*–*C*). This relative difference indicated decreased ability of IκBε knock-out cells to maintain robust oscillations. Further changes in parameter values caused termination of NF-κB oscillations in the IκBε knock-out cells, but not in WT (Fig. S21).

Heterogeneity of NF-κB Signaling Minimizes Fluctuations in Tissue-Level Paracrine Levels. Temporal and spatial coordination of tissue during an inflammatory response is largely controlled by secretion of paracrine factors by various cell types including fibroblasts (10, 27). Cytokines such as TNFα are early transcriptional targets of NF-κB (28). This represents an important intercellular positive feedback loop that reinforces activation of the system (Fig. 5*A*). Although this paracrine/autocrine signaling can contribute to amplification and propagation of inflammatory signals (11), this class of positive feedback motif has been suggested to decrease the robustness to perturbations and promote instability (20, 29, 30). Therefore, asynchronous NF-κB oscillations may reduce population-level fluctuations in cytokine production, whereas synchronous NF-κB oscillations might lead to an increased risk of uncontrolled inflammatory responses occurring, such as in septic shock (31).

We showed that altering the timing of the dual IκB feedback motif had a substantial effect on the level of cellular heterogeneity (Fig. 3). The resulting population level kinetics of NF-κB varied from a strongly damped (in WT) to very persistent (5-min delay in IκBε transcriptional initiation) oscillations (Fig. 5*B*). Therefore, we asked whether the timing of the dual IκB negative motif might affect the population level dynamics of a putative paracrine signal (e.g., a cytokine, such as TNFα). We built a model to simulate the regulation of the putative NF-κB-inducible paracrine gene (using an open feedback loop) and then studied simulated single cell paracrine oscillations (*SI Appendix*). Many paracrine gene products appear to have short half-lives [for instance 10-min mRNA (10) and 6-min protein half-life of TNFα (24, 32)]. As a consequence, when single cell dynamics were simulated using short mRNA and protein half-lives for the putative paracrine factor, the output levels of the protein showed significant fluctuations, which were directed by the NF-κB oscillations. Simulated data show that at the population level, the degree of cell-to-cell synchrony would significantly affect the degree of fluctuation in the average paracrine protein level (Fig. 5 *C* and *D*). Under these circumstances, our simulations suggest that the IκB dual delayed negative feedback motif may be responsible for smoothing population-level fluctuations in paracrine expression. This effect was exemplified by very broad bivariate distributions of peak amplitude and timing in WT, when compared with the IκBε knock-out, or the system with an altered delay time (Fig. 5*E*). This analysis showed that altering the relative delay of IκBε in the dual IκB negative feedback motif might promote persistent population-level fluctuations in paracrine signaling. This could potentially be very important across a tissue for minimizing potentially damaging peaks in cytokine levels that could lead to out-of-control inflammation.

Discussion

Understanding how the topology of genetic networks contributes to the emergence of biological function is a fundamental problem in systems biology (20, 33, 34). Topological complexity is exemplified by the NF-κB signaling network, which critically regulates not only the fate of individual cells but also overall population responses during inflammation (7).

In this study we analyzed the functional role of the dual-delayed IκB negative feedback motif in NF-κB signaling. We showed that this motif is critical in the maintenance of robust single cell

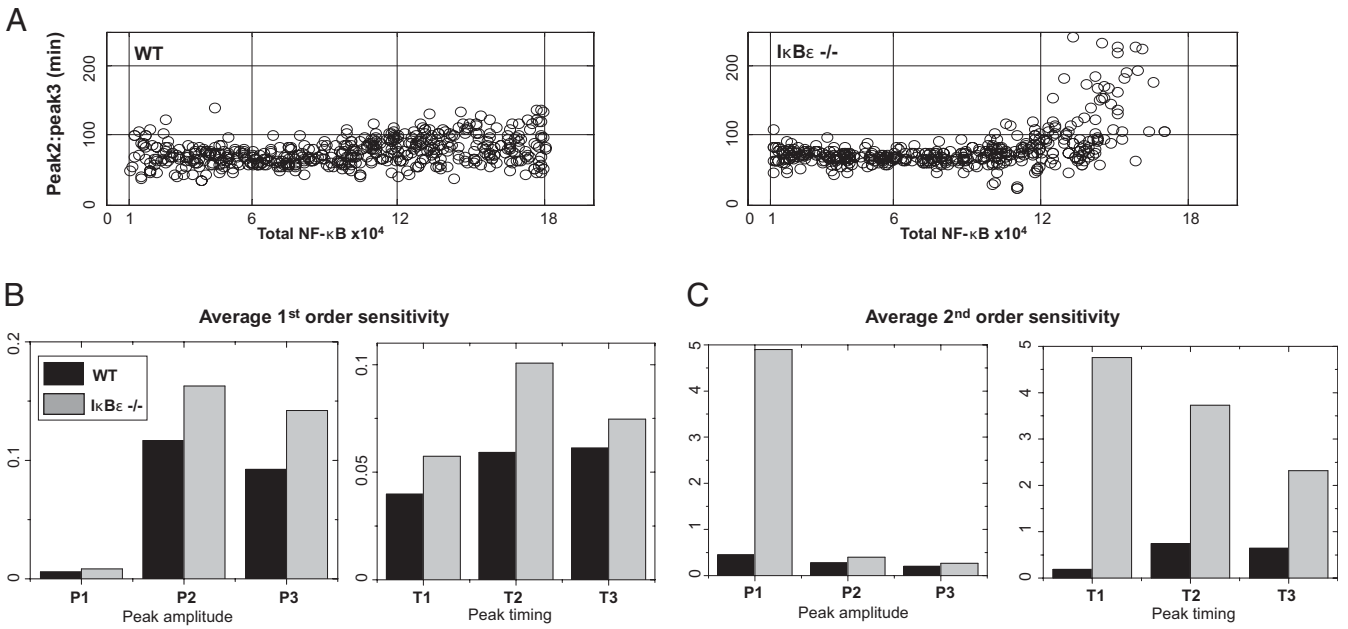

Fig. 4. IκBε feedback decreases single cell sensitivity to parameter variation. (*A*) Correlation between the NF-κB expression level and peak2-to-peak3 oscillation timing. Model simulations (500 single cells) for WT (*Left*) and IκBε$^{-/-}$ (*Right*) with the cellular NF-κB expression level uniformly distributed on the interval from 10,000–180,000 molecules. (*B* and *C*) Average sensitivity of nuclear NF-κB timing and amplitudes in WT and IκBε$^{-/-}$. Shown are averages of individual sensitivity coefficients normalized by the number of model parameters, Eq. **S8**, calculated for amplitudes (peak1, peak2, peak3) and peak timings (peak1 timing, peak2 timing, peak3 timing) of nuclear NF-κB. Forty-seven system parameters (in WT) and 33 parameters in IκBε$^{-/-}$ were independently changed twofold in both directions with respect to the nominal value (500 simulated cells per parameter change). (*B*) Average first-order (mean) sensitivity of peak amplitudes (*Left*) and timing (*Right*). (*C*) Average second-order (variability of) sensitivity of peak amplitudes (*Left*) and timing (*Right*).

oscillations in response to inflammatory cues by decreasing system sensitivity to parameter variation (Fig. 4). We also showed that the timing of the delayed IκB feedback was optimized to maximize the heterogeneity of NF-κB oscillation phasing between individual cells (Fig. 3). Through the simulation of a putative paracrine feedback, we predict that this heterogeneity would be recapitulated by the temporal heterogeneity of paracrine signal secretion by single cells, thus minimizing population-level paracrine fluctuations (Fig. 5). We therefore hypothesize that the NF-κB signaling system is optimized to minimize fluctuations in tissue-level responses and to promote tissue robustness and coordination through generation of cellular heterogeneity.

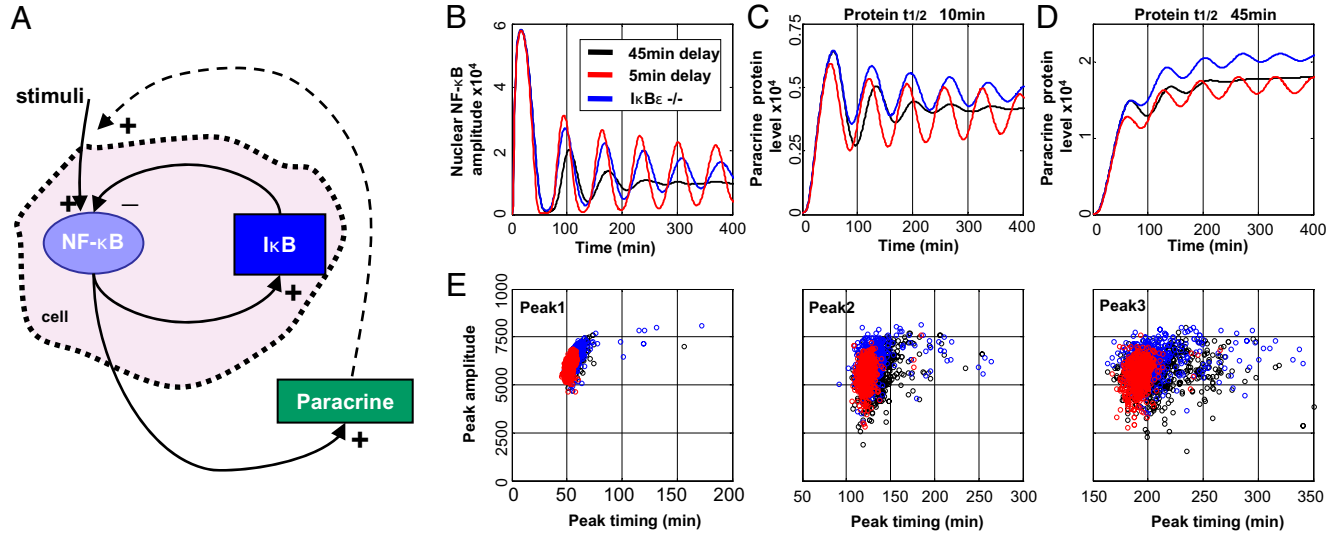

Fig. 5. Cellular heterogeneity minimizes fluctuations in tissue-level paracrine secretion (*A*) Schematic representation of a putative feedback loop due to paracrine signaling. (*B–E*) Analysis of paracrine signaling in the open loop (dashed line in *A* disconnected in the model). The model incorporates regulation of a putative diploid paracrine gene using parameters that match the dynamics of TNFα transcription and translation. The simulations shown are based on 500 cells. (*B*) Average nuclear NF-κB levels for 45-min delay (in black) and 5-min delay (in red) in IκBε transcription as well as IκBε$^{-/-}$ (in blue). (*C*) Average levels of paracrine protein, color-coded as in *B*. Ten-minute mRNA and protein half-life assumed. (*D*) Average levels of paracrine protein, color-coded as in *B*. The mRNA and protein half-lives are assumed to be 10 min and 45 min, respectively. (*E*) Distribution of peak timing and amplitude of paracrine protein, for data in *C* (color coding as in *B*).

Our data suggest that the network topology of the NF-κB signaling system is stimulus-dependent. In contrast to treatment with cytokines TNFα and IL-1β, the synthetic stimulus PMA failed to induce the 45-min time delay between transcription of IκBα and IκBε genes (Fig. 1 *B–D*). It is predicted by our *in silico* analysis that this timing affects the cellular heterogeneity of NF-κB oscillations and the ability of single cells to induce NF-κB oscillations (Figs. 3 and 4 and Figs. S16, S17, S18 and S19). Therefore, we hypothesize that the topology of the NF-κB network has structurally evolved to allow generation of a stimulus-specific tissue-level phenotype, which is required for appropriate propagation of the inflammatory cues, while simultaneously maintaining functional responsiveness of individual cells through maintenance of single cell oscillations.

Inflammatory processes are dynamic (4) and often exhibit oscillatory behavior both at the individual cell [such as NF-κB (13) and Ca^{2+} (16)] as well as at the organism level [e.g., periodic fevers during malarial infection (35)]. Other systems also exhibit oscillatory dynamics including the tumor suppressor p53 (36, 37) and ERK, a regulator of cell proliferation (38). Both exhibit asynchronous oscillations at the single cell level, similar to the NF-κB system (albeit with a different periodicity, 5.5 h and 15 min, respectively). In one study, tissue level oscillations of p53 were shown to be relatively synchronous following treatment with high dose ionizing radiation [as visualized by whole body imaging of transgenic mice expressing a p53 luciferase reporter (39)]. These data might suggest the presence of positive tissue-level feedback. It remains to be seen whether this system might also have a similar dual-delayed negative feedback motif. The functional significance of the damped tissue-level kinetics has not been established before in other characterized oscillatory systems such as p53. This may reflect unique properties and functional requirements for inflammatory responses.

Heterogeneity is a common feature of cellular processes. For example, individual eukaryotic cells exhibit noisy bursts of transcription (40). Oscillations in ERK in single mammalian cells (38) and Crz1 in yeast (41) are extremely noisy. Cell division and apoptosis also exhibit extreme heterogeneity, which might be a common feature of important cellular systems and complex diseases including cancer (29). It has often been thought that dynamic biological systems may have evolved to maximize robustness through intercellular coordination and homogeneity. In contrast, we propose that network topology in key signaling and regulatory systems may have evolved to give biological stability in acute tissue level responses that are made up from the average of highly heterogeneous single cell processes. This raises the interesting concept that genes or proteins specifically involved in the generation of cellular heterogeneity might constitute an alternative class of drug target. For example, drugs to alter heterogeneity in cancer cells might render a greater proportion of cells susceptible to therapeutic intervention.

Materials and Methods

Materials. Recombinant mouse and human TNFα and IL-1β were supplied by Calbiochem. PMA was from Sigma. Tissue culture medium was supplied by Invitrogen and FCS was from Harlan Sera-Lab.

Cell Culture. WT MEF cells (received from Ron Hay, University of Dundee, Dundee, United Kingdom) and SK-N-AS cells were grown as described previously (12).

qRT-PCR. Cells were seeded in 60-mm tissue culture dishes at 350,000 (MEF) or 500,000 (SK-N-AS) per dish and grown in an humidified atmosphere and 5% CO_2, and stimulated 24 h postplating with 10 ng/mL of TNFα, 10 ng/mL IL-1β or 100 μM of PMA. RNA was isolated using the RNeasy Mini Kit (Qiagen) and quantified with the Nanodrop ND-1000 Spectrophotometer (Thermo Fisher Scientific). 1 μg of total RNA from each sample was reverse transcribed using the SuperScript Vilo cDNA synthesis kit (Invitrogen). For qRT-PCR, 10 ng cDNA were used per reaction (total 20 μL), with DNA amplified with Lightcycler 480 Sybr Green 1 Master Mix (Roche). Relative quantification of gene expression was obtained by using the gene encoding Cyclophilin A as an endogenous control. Primer sequences for SK-N-AS samples were described previously (12), and MEF primer sequences were (5′-3′); IκBα forward ACAGGGTAACCTACCAAGGC and reverse CTGCTGTATCCGGGTACTTG, IκBε forward CTGTGCTGAATGTAGAAGA and reverse CATAGCAGTGGTTTGCCGGA, Cyclophilin A forward GCCGCGTCTCCTTCGA and reverse CGAAAGTTTTCTGCTGTCTTTGG.

Fluorescence Microscopy. Confocal microscopy was carried out as described previously (12) using a 40× objective. Cells were treated with 10 ng/mL of TNFα or IL-1β, and 16 μM of PMA 24 h posttransfection. CellTracker version 0.6 was used for data extraction (42). For RelA fusion proteins, mean fluorescence intensities were calculated for each time point for both nuclei and cytoplasm then nuclear:cytoplasmic (N:C) fluorescence intensity ratios were determined.

Mathematical Modeling. In this work, we extended (*SI Appendix*) our previously described three-feedback stochastic model of NF-κB signaling network (12). The current model was fitted to data in MEF cells (12, 17, 18, 22–24) obtained for saturated doses of TNFα (above 1 ng/mL) and incorporates a kinase IKKK in the transduction pathway leading to IKK activation (17).

The mathematical representation consists of coupled chemical reactions describing formation, dissociation and degradation of molecular complexes, transport between cellular compartments, transcription, translation, and regulation of gene activity. To aid model simulations, we developed a hybrid simulation algorithm that involves partitioning into fast and slow reactions (43) and subsequently considers a nonMarkovian delay introduced by transcription of IκBε gene (44). Stochasticity in the model arises because there are only two copies of IκBα, IκBε, and A20 feedback genes (3). We assumed that the probability of transcription factor binding at the promoter was proportional to the amount of nuclear NF-κB, whereas the dissociation probability depends on the level of nuclear IκBs (45). These probabilities imply that a single model simulation is a specific realization of an underlying stochastic process and therefore is directly comparable to the single-cell time-lapse microscopy data (12, 13). Population-level responses are recapitulated by ensemble averages.

Mathematical models were implemented and simulated in Matlab R2009a environment. Equation files and simulation routines are available for downloading at http://www.liv.ac.uk/bio/research/groups/cci/.

ACKNOWLEDGMENTS. N. Perkins, R. Beynon, R. Bowers, D. Kell, R Bearon, H. Rees, P. Rudland, and M. Kimmel commented on the manuscript; C. Horton contributed to model development. We thank A. Haoffmann for permission to reproduce previously published material in the supplementary information. Financial support was provided by Medical Research Council (G0500346), Biotechnology and Biological Sciences Research Council (BBF0059381/BBF0058141), Engineering and Physical Sciences Research Council (DR-Senior Fellowship, EP/C544587/1, GR/S29256/01), and European Union BIOSIM Network Contract 005137.

1. Cai L, Friedman N, Xie XS (2006) Stochastic protein expression in individual cells at the single molecule level. *Nature* 440:358–362.
2. Elowitz MB, Levine AJ, Siggia ED, Swain PS (2002) Stochastic gene expression in a single cell. *Science* 297:1183–1186.
3. Raj A, Peskin CS, Tranchina D, Vargas DY, Tyagi S (2006) Stochastic mRNA synthesis in mammalian cells. *PLoS Biol* 4:1707–1719.
4. Stark J, Chan C, George AJ (2007) Oscillations in the immune system. *Immunol Rev* 216:213–231.
5. Indic P, Schwartz WJ, Herzog ED, Foley NC, Antle MC (2007) Modeling the behavior of coupled cellular circadian oscillators in the suprachiasmatic nucleus. *J Biol Rhythms* 22:211–219.
6. Liu AC, et al. (2007) Intercellular coupling confers robustness against mutations in the SCN circadian clock network. *Cell* 129:605–616.
7. Hayden MS, Ghosh S (2008) Shared principles in NF-kappaB signaling. *Cell* 132:344–362.
8. Sée V, Rajala NK, Spiller DG, White MR (2004) Calcium-dependent regulation of the cell cycle via a novel MAPK—NF-kappaB pathway in Swiss 3T3 cells. *J Cell Biol* 166:661–672.
9. Ward C, et al. (1999) NF-kappaB activation is a critical regulator of human granulocyte apoptosis in vitro. *J Biol Chem* 274:4309–4318.
10. Hao S, Baltimore D (2009) The stability of mRNA influences the temporal order of the induction of genes encoding inflammatory molecules. *Nat Immunol* 10:281–288.
11. Lee TK, et al. (2009) A noisy paracrine signal determines the cellular NF-kappaB response to lipopolysaccharide. *Sci Signal* 2:ra65.
12. Ashall L, et al. (2009) Pulsatile stimulation determines timing and specificity of NF-kappaB-dependent transcription. *Science* 324:242–246.

13. Nelson DE, et al. (2004) Oscillations in NF-kappaB signaling control the dynamics of gene expression. *Science* 306:704–708.
14. Friedrichsen S, et al. (2006) Tumor necrosis factor-alpha activates the human prolactin gene promoter via nuclear factor-kappaB signaling. *Endocrinology* 147:773–781.
15. Sung MH, et al. (2009) Sustained oscillations of NF-kappaB produce distinct genome scanning and gene expression profiles. *PLoS One* 4:e7163.
16. Dolmetsch RE, Lewis RS (1994) Signaling between intracellular Ca2+ stores and depletion-activated Ca2+ channels generates [Ca2+]i oscillations in T lymphocytes. *J Gen Physiol* 103:365–388.
17. Hoffmann A, Levchenko A, Scott ML, Baltimore D (2002) The IkappaB-NF-kappaB signaling module: Temporal control and selective gene activation. *Science* 298:1241–1245.
18. Kearns JD, Basak S, Werner SL, Huang CS, Hoffmann A (2006) IkappaBepsilon provides negative feedback to control NF-kappaB oscillations, signaling dynamics, and inflammatory gene expression. *J Cell Biol* 173:659–664.
19. Kim D, Kolch W, Cho KH (2009) Multiple roles of the NF-kappaB signaling pathway regulated by coupled negative feedback circuits. *FASEB J* 23:2796–2802.
20. Alon U (2007) Network motifs: Theory and experimental approaches. *Nat Rev Genet* 8:450–461.
21. Lipniacki T, Puszynski K, Paszek P, Brasier AR, Kimmel M (2007) Single TNFalpha trimers mediating NF-kappaB activation: Stochastic robustness of NF-kappaB signaling. *BMC Bioinformatics* 8:376.
22. Lee EG, et al. (2000) Failure to regulate TNF-induced NF-kappa B and cell death responses in A20-deficient mice. *Science* 289:2350–2354.
23. Werner SL, Barken D, Hoffmann A (2005) Stimulus specificity of gene expression programs determined by temporal control of IKK activity. *Science* 309:1857–1861.
24. Werner SL, et al. (2008) Encoding NF-kappaB temporal control in response to TNF: Distinct roles for the negative regulators IkappaBalpha and A20. *Genes Dev* 22:2093–2101.
25. Barken D, et al. (2005) Comment on "Oscillations in NF-kappaB signaling control the dynamics of gene expression". *Science* 308:52.
26. Ihekwaba AE, Broomhead DS, Grimley RL, Benson N, Kell DB (2004) Sensitivity analysis of parameters controlling oscillatory signalling in the NF-kappaB pathway: The roles of IKK and IkappaBalpha. *Syst Biol (Stevenage)* 1:93–103.
27. Bradley JR (2008) TNF-mediated inflammatory disease. *J Pathol* 214:149–160.
28. Tian B, Nowak DE, Brasier AR (2005) A TNF-induced gene expression program under oscillatory NF-kappaB control. *BMC Genomics* 6:137.
29. Kitano H (2004) Cancer as a robust system: Implications for anticancer therapy. *Nat Rev Cancer* 4:227–235.
30. Stelling J, Sauer U, Szallasi Z, Doyle FJ, 3rd, Doyle J (2004) Robustness of cellular functions. *Cell* 118:675–685.
31. Tracey KJ, et al. (1987) Anti-cachectin/TNF monoclonal antibodies prevent septic shock during lethal bacteraemia. *Nature* 330:662–664.
32. Beutler BA, Milsark IW, Cerami A (1985) Cachectin/tumor necrosis factor: Production, distribution, and metabolic fate in vivo. *J Immunol* 135:3972–3977.
33. Brandman O, Meyer T (2008) Feedback loops shape cellular signals in space and time. *Science* 322:390–395.
34. Milo R, et al. (2002) Network motifs: Simple building blocks of complex networks. *Science* 298:824–827.
35. Kwiatkowski D, Nowak M (1991) Periodic and chaotic host-parasite interactions in human malaria. *Proc Natl Acad Sci USA* 88:5111–5113.
36. Geva-Zatorsky N, et al. (2006) Oscillations and variability in the p53 system. *Molecular Systems Biology* 2:1–13.
37. Lahav G, et al. (2004) Dynamics of the p53-Mdm2 feedback loop in individual cells. *Nat Genet* 36:147–150.
38. Shankaran H, et al. (2009) Rapid and sustained nuclear-cytoplasmic ERK oscillations induced by epidermal growth factor. *Mol Syst Biol* 5:332.
39. Hamstra DA, et al. (2006) Real-time evaluation of p53 oscillatory behavior in vivo using bioluminescent imaging. *Cancer Res* 66:7482–7489.
40. Raj A, van Oudenaarden A (2008) Nature, nurture, or chance: Stochastic gene expression and its consequences. *Cell* 135:216–226.
41. Cai L, Dalal CK, Elowitz MB (2008) Frequency-modulated nuclear localization bursts coordinate gene regulation. *Nature* 455:485–490.
42. Shen H, et al. (2006) Automated tracking of gene expression in individual cells and cell compartments. *J R Soc Interface* 3:787–794.
43. Haseltine EL, Rawlings JB (2002) Approximate simulation of coupled fast and slow reactions for stochastic chemical kinetics. *J Chem Phys* 117:6959–6969.
44. Cai XD (2007) Exact stochastic simulation of coupled chemical reactions with delays. *J Chem Phys* 126:124108.
45. Bergqvist S, et al. (2009) Kinetic enhancement of NF-kappaBxDNA dissociation by IkappaBalpha. *Proc Natl Acad Sci USA* 106:19328–19333.